JOURNAL OF ENVIRONMENTAL SCIENCES 49 (2016) 74–85

Available online at www.sciencedirect.com

ScienceDirect

www.elsevier.com/locate/jes

JES JOURNAL OF ENVIRONMENTAL SCIENCES

www.jesc.ac.cn

Review

Recent progress of arsenic adsorption on TiO_2 in the presence of coexisting ions: A review

*Li Yan, Shan Hu, Chuanyong Jing**

1. *State Key Laboratory of Environmental Chemistry and Ecotoxicology, Research Center for Eco-Environmental Sciences, Chinese Academy of Sciences, Beijing 100085, China. E-mail: jilin2008yanli@163.com*
2. *University of Chinese Academy of Sciences, Beijing 100049, China*

ARTICLE INFO

Article history:
Received 7 April 2016
Revised 12 July 2016
Accepted 22 July 2016
Available online 1 August 2016

Keywords:
Arsenic
TiO_2 adsorbent
Coexisting ions
CD-MUSIC
PHREEQC
Regeneration

ABSTRACT

Arsenic (As)-contaminated wastewater and groundwater pose a pressing environmental issue and worldwide concern. Adsorption of As using TiO_2 materials, in combination with filtration, introduces a promising technology for the treatment of As-contaminated water. This review presents an overview on the recent progress of the application of TiO_2 for removal of As from wastewater and groundwater. The main focus is on the following three pressing issues that limit the field applications of TiO_2 for As removal: coexisting ions, simulation of breakthrough curves, and regeneration and reuse of spent TiO_2 materials. We first examined how the coexisting ions in water, especially high concentrations of cations in industrial wastewater, affect the efficacy of As removal using the TiO_2 materials. We then discussed As breakthrough curves and the effect of compounded ions on the breakthrough curves. We successfully simulated the breakthrough curves by PHREEQC after integrating the CD-MUSIC model. We further discussed challenges facing the regeneration and reuse of TiO_2 media for practical applications. We offer our perspectives on remaining issues and future research needs.

Introduction

As a versatile material, TiO_2 has been widely used for arsenic (As) removal, as reported in a previous review (Guan et al., 2012). Recently, the number of publications and citations regarding the use of TiO_2 for As adsorption has increased significantly (Fig. 1). Many efforts have attempted to synthesize effective TiO_2-based materials including nanocrystalline TiO_2 particles (Dutta et al., 2004; Guo et al., 2013; Jegadeesan et al., 2010; Kocabas-Atakli and Yurum, 2013; Nabi et al., 2009; Pena et al., 2005; Xu and Meng, 2009), hydrous TiO_2 (Pirila et al., 2011; Sun et al., 2013; Xu et al., 2010), titanate nanotubes (Niu et al., 2009; Wu et al., 2013), granular TiO_2 (Bang et al., 2005; Cui et al., 2015a; Hu et al., 2015a; Yan et al., 2015), TiO_2-impregnated chitosan beads (Miller and Zimmerman, 2010), and TiO_2-coated sand (Nabi et al., 2009). The performances of those TiO_2-based materials are summarized in Table 1. Initially, TiO_2 was utilized mainly as a fine powder, which exhibits well-known limitations in practical applications. Solving the problem of TiO_2 powder exhibiting high hydraulic loss in a fixed-bed column (Hristovski et al., 2007), requires laborious solid/liquid separation for regeneration (Luo et al., 2010), and includes the possible leakage of As-adsorbed nano-sized TiO_2. Granular TiO_2 (0.18–0.83 mm),

* *Corresponding author*. E-mail: cyjing@rcees.ac.cn (Chuanyong Jing).

http://dx.doi.org/10.1016/j.jes.2016.07.007

mesoporous titania beads (0.5 mm) (Dwivedi et al., 2012), and TiO_2-impregnated chitosan beads (1.0 mm) with a large particle size that can be operated in fixed-bed columns have been developed in recent years for As removal. Due to its high adsorption efficiency, ability to be regenerable and reusable, cost-effectiveness, and feasible operation (Chen and Mao, 2007; Luo et al., 2010; Yan et al., 2015), TiO_2 is becoming a promising material in field filtration of As tainted waters.

Though there are many successful applications of TiO_2 in As remediation, three pressing issues still remain, which limit its practical application in field filtration. First, the impacts of coexisting ions on As removal at the TiO_2 surface are not fully understood, especially for cations with high concentrations in industrial wastewater (Hu et al., 2015b). Second, the simulation of As breakthrough curves in TiO_2 filtration columns is far from satisfactory, and the methods of obtaining the parameters from batch adsorptions in the laboratory used to accurately predict the field filtration need more effort to decipher (Cui et al., 2015a; Hu et al., 2015a). Third, the regeneration and reuse of spent TiO_2 media is still a challenge for the practical application of TiO_2 (Arumugam et al., 2013; Bang et al., 2005; Hu et al., 2015a; Yan et al., 2015).

This paper reviews the recent progress of TiO_2 applications for treating real As-contaminated waters, focusing on industrial wastewater containing high concentrations of As and coexisting heavy metals, as well as groundwater which experiences a combined ion effect from the presence of other ions. A survey of the influence that coexisting ions have on As removal at the TiO_2 surface is discussed. Then, a connection of laboratory experiments with field filtration is established by evaluating the effect of the compounded ions (Fig. 2). Finally, a future perspective is discussed and an outlook is featured.

1. Compounding ion effects on As adsorption to TiO_2

1.1. Cd at high concentrations in industrial wastewater

Smelting wastewater is usually coupled with high concentrations of As and Cd, which presents a major challenge to the environment (Bian et al., 2012; Hao et al., 2015; Liao et al., 2016; Roussel et al., 2000). TiO_2 has been investigated to simultaneously remove high concentrations of As(III) and Cd from metallurgical wastewater (Luo et al., 2010; Yan et al., 2015). A strategy for determining As(III) and Cd treatability was implemented in three successive fixed-bed columns, and the initial concentration averages of 2590 mg/L As(III) and 12 mg/L Cd in the raw water were reduced to below discharge limit in the effluent each time for 10 treatment cycles (Fig. 3). Though extensive studies have been motivated to investigate the interaction of cationic metals and anionic ligands on metal oxide surfaces (Grafe et al., 2004, 2008; Jiang et al., 2013; Ler and Stanforth, 2003), the molecular-level interactions between cationic Cd and neutrally charged As(III) on the TiO_2 surface are poorly understood.

The formation of ternary surface complexes is considered the primary uptake mechanism for As(III) and Cd on TiO_2. A systematical study performed by Hu et al. (2015b) indicated that the formation of ternary surface complexes was dependent on the mole ratio of As(III) to Cd. At low As(III) and Cd concentrations (Cd = 3.11 mmol/L, As/Cd ratio below 0.5), both As(III) and Cd adsorbed onto the TiO_2 surface as bidentate binuclear structures. With an increase in the As/Cd ratio from 0.5 to 15.8, the adsorbed Cd desorbed from the surface and formed a Cd–As(III)–TiO_2 ternary surface complexion with the adsorbed As(III) serving as the bridging molecule and occupying more Ti sites (Fig. 4). Synergistic adsorption of As(III) and Cd on TiO_2 was observed after the formation of ternary surface complexes. Cd adsorption increased from a range of 4.0–13.4 μmol/m^2 in the Cd–TiO_2 binary system to 9.7–15.2 μmol/m^2 for simulated wastewater (As(III)/Cd = 2.0) and 17.1–25.2 μmol/m^2 for smelting wastewater (As(III)/Cd = 10.4) in the Cd–As(III)–TiO_2 ternary system. As(III) adsorption increased from 1.6 μmol/m^2 in the As(III)–TiO_2 binary system to 6.2 μmol/m^2 in the ternary Cd–As(III)–TiO_2 system (Fig. 5a–b).

Results from ongoing studies involving the co-adsorption of As(V) and Cd on TiO_2 indicate that ternary surface complexes and surface precipitates can form depending on the As(V)/Cd mole ratio. With low initial As(V) (0.13 mmol/L) and Cd concentrations (0.07 mmol/L), only ternary surface complexes of Cd–As(V)–TiO_2 were observed. By increasing As(V) to 2.0 mmol/L and Cd concentrations to 3.11 mmol/L, different surface precipitates formed. With an initial Cd concentration of 3.11 mmol/L, and As/Cd = 0.5 at pH 5, only the precipitate of $Cd_3(AsO_4)_2$ was found; while for As/Cd ratio range of 2–10, both $Cd_3(AsO_4)_2$ and $Cd_5H_2(AsO_4)$ $4H_2O$ compounds existed. At pH 7, both of these precipitates existed for all samples with As/Cd ratio range of 0.5–10. Only a small amount of $Cd_5H_2(AsO_4)$ $4H_2O$ existed, a

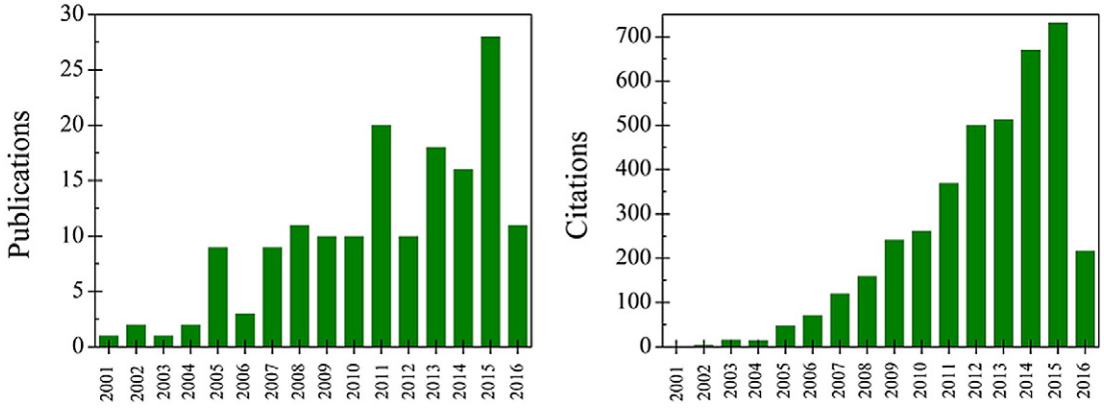

Fig. 1 – The number of publications and citations on arsenic removal using TiO_2 in the most recent 20 years through the Web of Science™ Core Collection. The keywords for searching are "arsenic" and "TiO_2."

Table 1 – Summary of arsenic adsorption on TiO_2 and TiO_2-based materials.

TiO_2	Properties			Reaction conditions			Adsorption capacity (mg/g)	Reference
	Particle size (nm)	Specific surface area (cm^2/g)	pHpzc	As concentration (mg/L)	pH	Adsorbent (g/L)		
Nanocrystalline TiO_2	6	330	5.8	$[As(III)]_e$ = 45	7	1	>37.5	Pena et al. (2005)
				$[As(V)]_e$ = 45	7	1	>37.5	
HM	4.6	336	5.3	$[As(III)]_0$ = 0.31–3450	7	5	136	Yan et al. (2016)
				$[As(V)]_0$ = 0.32–4484	7	5	140	
JR05	7.5	167	6.5	$[As(III)]_0$ = 0.31–3450	7	5	138	
				$[As(V)]_0$ = 0.32–4484	7	5	144	
TG01	18.2	71	6.1	$[As(III)]_0$ = 0.31–3450	7	5	71	
				$[As(V)]_0$ = 0.32–4484	7	5	106	
TiO_2	6.6	287.8		$[As(III)]_0$ = 0–80	7	1	30.0	Xu and Meng (2009)
				$[As(V)]_0$ = 0–80	7	1	30.5	
	7.0	255.9		$[As(III)]_0$ = 0–80	7	1	25.4	
				$[As(V)]_0$ = 0–80	7	1	28.0	
	10.5	141.3		$[As(III)]_0$ = 0–80	7	1	15.1	
				$[As(V)]_0$ = 0–80	7	1	18.0	
	14.8	96.0		$[As(III)]_0$ = 0–80	7	1	8.52	
				$[As(V)]_0$ = 0–80	7	1	9.86	
	30.1	25.7		$[As(III)]_0$ = 0–80	7	1	2.16	
				$[As(V)]_0$ = 0–80	7	1	3.62	
Nanoadsorbent	7.97			$[As(III)]_0$ = 0.1–20	6	0.5	16.98	Kocabas-Atakli and Yurum (2013)
Amorphous TiO_2		409	4.5	$[As(III)]_0$ = 0.2–50	7	0.2	66.8	Jegadeesan et al. (2010)
				$[As(V)]_0$ = 0.2–50	7	0.2	19.0	
Hombikat UV100	<10	334	6.2	$[As(III)]_e$ = ~31.9	9		43.1 ± 5.2	Dutta et al. (2004)
				$[As(V)]_e$ = ~37.5	4		22.5 ± 5.9	
Degussa P25	~30	~55	6.9	$[As(III)]_e$ = ~39.8	9		3.9 ± 2.4	
				$[As(V)]_e$ = ~37.5	4		4.6 ± 0.7	
polymer–TiO_2	<25	45–55		$[As]_0$ = 10–1000	6	6	144.0–162.3	Urbano et al. (2015)
GPR TiO_2	325			$[As(III)]_0$ = 5–90	7.6	1	17.0–18.8	Nabi et al. (2009)
				$[As(V)]_0$ = 5–90	7.6	1	19.0	
Pure TiO_2	108			$[As(III)]_0$ = 5–90	7.6	1	18.0–20.3	
				$[As(V)]_0$ = 5–90	7.6	1	20.4	
Hydrous TiO_2	3–8	312	3.8	$[As(III)]_0$ = 0–170	7	0.5	83	Xu et al. (2010)
				$[As(III)]_0$ = 0–170	9	0.5	96	
Hydrous TiO_2	10.8	280	4.8	$[As(III)]_0$ = 0.2–8.5	4–6		25.8–32.1	Pirila et al. (2011)
				$[As(V)]_0$ = 0.2–8.5	4–6		22.0–33.4	
Ti hydroxide				$[As(III)]_e$ = 4.1	7	2	500	Sun et al. (2013)
3D titanium dioxide	200–350	202.6	3.76	$[As(V)]_e$ = ~97.2	4	0.1	59.7	Guo et al. (2013)
TiO_2 nanotube arrays	4 μm	49.5	5.39	$[As(III)]_0$ = 0.5–30	7	0.9	28.9	Wu et al. (2013)
				$[As(V)]_0$ = 0.5–30	7	0.9	24.7	
Granular TiO_2	0.15–0.6 mm	250.7	5.8	$[As(III)]_0$ = 0.4–80	7	1	32.4	Bang et al. (2005)
				$[As(V)]_0$ = 0.4–80	7	1	41.4	
Granular TiO_2	0.18–0.25 mm	196	5.8	$[As(III)]_0$ = 1–800	8.2	1	93.0	Hu et al. (2015a)
				$[As(V)]_0$ = 1–800	8.2	1	35.2	
Granular TiO_2	0.25–0.38 mm	196	5.8	$[As(III)]_0$ = 0.39–2460	5	2.5	145	Yan et al. (2015)
				$[As(III)]_0$ = 0.39–2460	7	2.5	160	
Granular TiO_2	0.38–0.83 mm	196	5.8	$[As(III)]_e$ = ~430	8.2	1	106.4	Cui et al. (2015a)
				$[As(V)]_e$ = ~580	8.2	1	38.3	
TiO_2-impregnated chitosan bead	~1 mm	0.56	7.25	$[As(III)]_0$ = 0.1–10	9.2	0.625	2.10	Miller and Zimmerman (2010)
				$[As(V)]_0$ = 0.1–10	7.7	0.625	2.05	
		3.06 with UV irradiation		$[As(III)]_0$ = 0.1–10	6.6 (UV)	0.625	3.54	
				$[As(V)]_0$ = 0.1–10	7.0 (UV)	0.625	2.99	
TiO_2-coated sand				$[As(III)]_0$ = 0.1	7.6	4	0.014	Nabi et al. (2009)
				$[As(V)]_0$ = 0.1	7.6	4	0.022	
TiO_2–SiO_2–polyacrylonitrile	1.0–2.0 mm	170		$[As(III)]_e$ = 2.85	8	1	4.90	Nilchi et al. (2011)

Subscripts "e" and "0" represent equilibrated and initial arsenic concentrations, respectively.

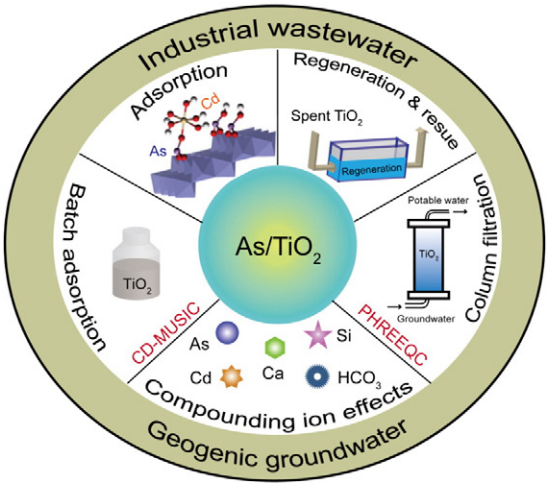

Fig. 2 – Picture for As removal using TiO_2.

large portion of it being an amorphous Cd–As(V) precipitate at pH 9. The formation of ternary surface complexes and surface precipitates enhanced the synergetic adsorption of As(V) and Cd on TiO_2. Cd adsorption increased from 13.0 μmol/m^2 in the binary Cd–TiO_2 system to 15.4 μmol/m^2 in the ternary Cd–As(V)–TiO_2 system. For As(V) adsorption, this value was significantly enhanced from 5.3 to 14.3 μmol/m^2 (Fig. 5c–d).

These results demonstrate that concentrations of coexisting metals and pH conditions can significantly influence the wastewater treatment efficiency by changing the reaction mechanism of As and coexisting heavy metals with solid-water surfaces. A neutral pH condition and appropriate mole ratio are preferred to obtain a satisfactory removal efficiency. However, ensuring optimal removal remains a challenge due to the reality that most industrial wastewater exhibits a low pH of 1.0, and the fact that the As/Cd molar ratio in real wastewater is largely dependent on the associated industrial process.

1.2. Synergistic uptake mechanism for As and Cd on TiO_2

The formation of a ternary surface complexion in Cd–As(III)–TiO_2 system has been evidenced by multiple complementary techniques. A mass balance calculation predicted that Cd in smelting wastewater will occupy more than 50.4 μmol/m^2 sites with bidentate binuclear complexes if adsorption is the only removal mechanism. However, TiO_2 exhibited a theoretical site concentration of only 30.6 μmol/m^2. The lower availability of sites demonstrated that other mechanisms besides adsorption must contribute to the Cd removal (Grafe et al., 2004; Jiang et al., 2013). Synchrotron-based extended X-ray absorption fine structure (EXAFS) spectroscopy did not evidence any Cd–As(III) complexes in the raw water (Luo et al., 2010), but the ternary surface complexions Cd–As(III)–TiO_2 were shown to form on the TiO_2 surface (Hu et al., 2015b). The As K-edge spectra can only be fitted well with the addition of an extra As–Cd path at 3.48–3.62 Å. The confidence level for adding this path is in the range of 86.4%–98.2%, significantly higher than the required value of 67%, which confirms the appropriateness of adding As–Cd to the As–Ti path. *In-situ* attenuated total reflection Fourier transform infrared spectroscopy demonstrated that during co-adsorption of As(III) and Cd, the vibration of As(III)–OH at 816/cm disappeared due to the fact that Cd can occupy the Ti–O–As complex sites to form a Ti–O–As–O–Cd ternary complex, which was further confirmed by density functional theory calculations (Hu et al., 2015b).

The macroscopic observation for change of ζ potential by synergistic adsorption can be simulated with charge distribution multi-site complexation (CD-MUSIC) modeling under the constraint of molecular-level results (Hu et al., 2015b). The pHpzc of TiO_2 changed from initial 5.3 to 5.7 upon first Cd adsorption, and then decreased to 4.4 after As(III) was added to the system (Fig. 6a). Conversely, the pHpzc of TiO_2 first changed from 5.3 to 4.6 upon As(III) adsorption, and then increased to 5.2 after Cd was added to the above As(III)–TiO_2 adsorption system (Fig. 6b). This charge neutralization demonstrates the formation of ternary surface complexes, where the adsorbed As(III) can provide new sites for Cd adsorption. Therefore, the complexes of $Ti_2O_2AsO^{-5/3}$, $Ti_2O_2Cd^{-2/3}$, and

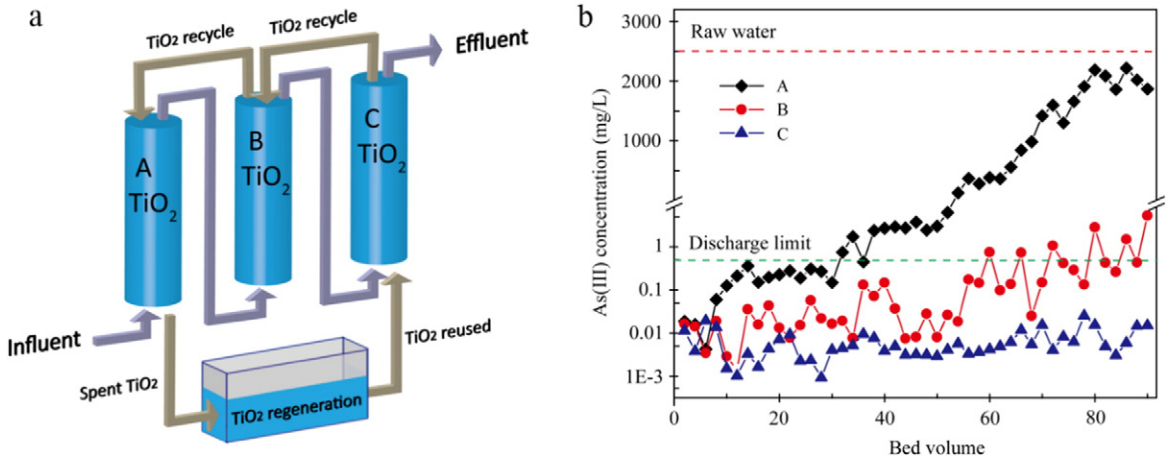

Fig. 3 – (a) Schematic flowchart for the proposed As-contaminated wastewater treatment process using granular TiO_2 columns. (b) As(III) breakthrough curves of three columns in series in a typical treatment cycle (Yan et al., 2015).

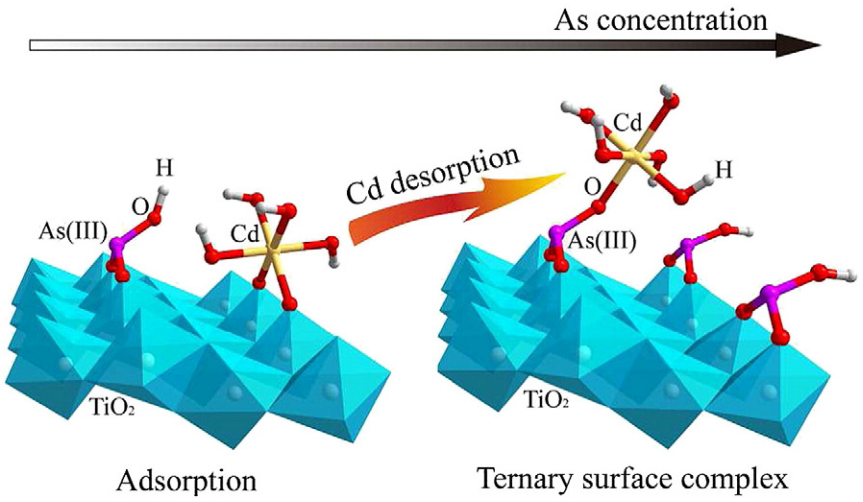

Fig. 4 – Surface complexation for As(III) and Cd co-adsorption on TiO_2 (Hu et al., 2015b).

$Ti_2O_2AsOCd^{1/3}$ were used to simulate binary As(III)–TiO_2, binary Cd–TiO_2, and ternary Cd–As(III)–TiO_2 adsorption systems, respectively.

For the system of As(V) adsorption on TiO_2, the pHpzc of TiO_2 changed from initial 5.3 to 3.4 upon As(V) adsorption, indicating the formation of inner-sphere complexes. For the system of As(V) and Cd co-adsorption on TiO_2, the pHpzc of TiO_2 changed from initial 5.3 to 4.1 (Fig. 6c), indicating the formation of a ternary Cd–As(V)–TiO_2 surface complex. The complexes $Ti_2O_2AsO_2^{-5/3}$ and $Ti_2O_2AsO_2Cd^{1/3}$ were used to simulate binary As(V)–TiO_2 and ternary Cd–As(V)–TiO_2 adsorption systems, respectively. The CD-MUSIC model described the following binary and ternary surface reactions:

$$\text{Binary Cd–TiO}_2 : 2\text{`TiOH}^{-1/3} + Cd^{2+} = \text{`Ti}_2O_2Cd^{-2/3} + 2H^+ \quad (1)$$

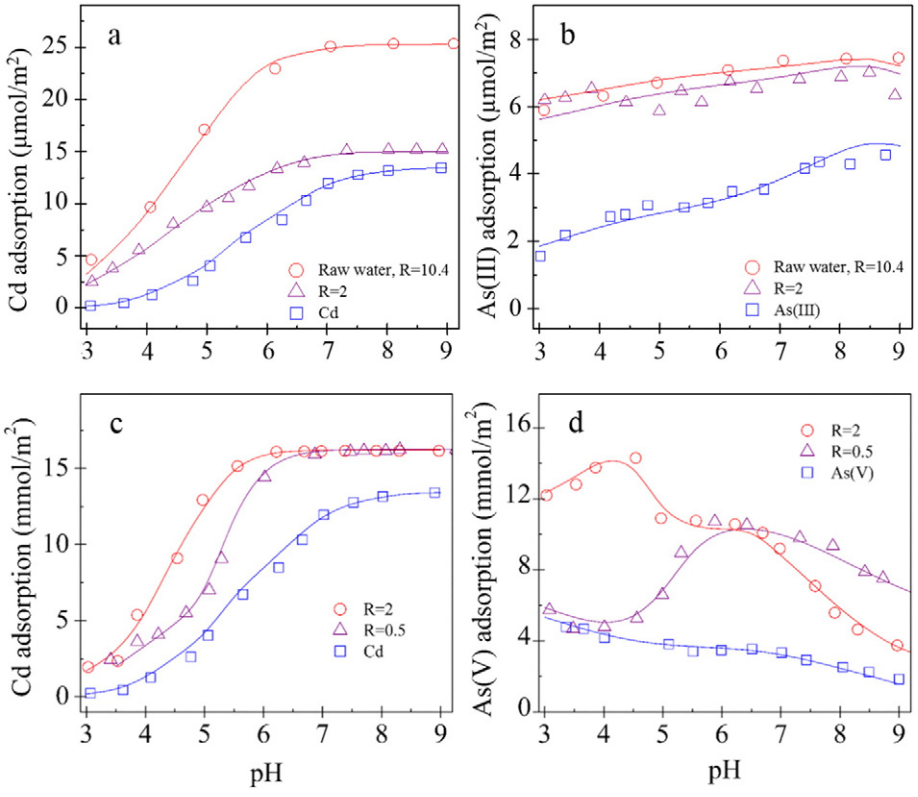

Fig. 5 – Experimental pH adsorption edges (symbols) and charge distribution multi-site complexation (CD-MUSIC) calculations (lines) of Cd (a) and As(III) (b) in simulated wastewater (molar ratio of As(III)/Cd(R) = 2, As(III) = 5.26 mmol/L) and copper smelting wastewater (R = 10.4, As(III) = 51.52 mmol/L) (Hu et al., 2015b). Experimental pH adsorption edges (symbols) and CD-MUSIC calculations (lines) of Cd (c) and As(V) (d) in simulated wastewater (molar ratio of As(V)/Cd, R = 0.5 and 2, Cd = 3.11 mmol/L).

$$\text{Binary As(III)–TiO}_2 : 2\text{`iOH}^{-1/3} + H_3AsO_3 = \text{`Ti}_2O_2AsO^{-5/3} + 2H_2O + H^+ \quad (2)$$

$$\text{Ternary Cd–As(III)–TiO}_2 : 2\text{`TiOH}^{-1/3} + H_3AsO_3 + Cd^{2+} = \text{`Ti}_2O_2AsOCd^{1/3} + 2H_2O + H^+ \quad (3)$$

$$\text{Binary As(V)–TiO}_2 : 2\text{`TiOH}^{-1/3} + AsO_4^{3-} + 2H^+ = \text{`Ti}_2O_2AsO_2^{-5/3} + 2H_2O \quad (4)$$

$$\text{Ternary Cd–As(V)–TiO}_2 : 2\text{`TiOH}^{-1/3} + AsO_4^{3-} + 2H^+ + Cd^{2+} = \text{`Ti}_2O_2AsO_2Cd^{1/3} + 2H_2O \quad (5)$$

The synergistic adsorption of As and Cd on TiO_2 *via* the formation of ternary surface complexes and surface precipitates further inhibited the metal release into the aqueous phase, contributing to its immobilization (Grafe et al., 2004, 2008; Jiang et al., 2013). Though much effort was put into studying the synergetic uptake mechanism of As adsorption on metal oxide surfaces with the influence of coexisting heavy metals, the results may be a case-by-case study due to the complicated contamination species and various solid-water interfaces.

1.3. Coexisting ions in geogenic groundwater

Besides cations with high concentrations in wastewater, cations such as calcium (Ca) and magnesium (Mg) in groundwater also have synergistic effects on As(V) adsorption due to electrostatic forces, while exhibiting negligible effects on As(III) (Cui et al., 2015a; Kanematsu et al., 2013; Stachowicz et al., 2008). Hu et al. (2015a) studied the interference of Ca toward As(V) molecular structures absorbed on TiO_2, and the results suggested the formation of a Ca–As(V)–TiO_2 ternary surface complex. The formation of a ternary complex can significantly increase the synergetic uptake of As(V) and Ca (Masue et al., 2007), and promote As attenuation in groundwater (Zhang et al., 2014). Though the coexisting Mg concentration (104.3 mg/L) was much higher than Ca (39.1 mg/L) in groundwater, the Ca adsorption density was higher than Mg (311 mg/g *vs.* 171 mg/g) in a study by Cui et al. (2015a). These interesting results may be attributed to the distinct adsorption behaviors, where Ca can strongly bond to the surface and form a Ca–As(V)–TiO_2 ternary complex.

In contrast to cations, As adsorption on metal oxides is sometimes suppressed in the presence of co-existing anionic and nonionic species. Niu et al. (2009) demonstrated that anions such as phosphate (P), silicate (Si), and sulfate (SO_4^{2-}) decreased As(V) adsorption on TiO_2-based materials (TN 180-1), but no evident competition was observed for As(III) removal; however, the reduced removal efficiency for both As(III) and As(V) *via* TiO_2 under competing ions was observed by Pena et al. (2005). Jegadeesan et al. (2010) reported that the presence of P (7 mg/L) and Si (20 mg/L) decreased As(III) adsorption to amorphous TiO_2 by 43.0%; whereas the As(V) adsorption capacity of amorphous TiO_2 was not affected by the presence of P, but declined by 29.1% in the presence of Si. The effects of nitrate (NO_3^-) and chloride (Cl^-) on As adsorption have been proven to be negligible (Ciardelli et al., 2008; Hu et al., 2015a). In another study by Cui et al. (2015a), bicarbonate (HCO_3^-) significantly inhibited As(V) adsorption by 52% from 5.0 to 2.4 mg/g, however, As(III) adsorption declined by only 8% on granular TiO_2. Deng et al. (2010) determined the influence of anions in groundwater on the adsorption of As(V) to a Ce–Ti oxide adsorbent, which followed the order of HPO_4^{2-} > HCO_3^- > SiO_3^{2-} > SO_4^{2-} ≈ NO_3^- > Cl^-. Liang et al. (2016) studied As retention and transport behavior in the presence of anionic and nonionic surfactants, and their results indicated that coexisting surfactants decreased As adsorption on ferrihydrite by up to 29.7%. The increase in As mobilization by organic matrix can be attributed to the formation of As-organic matter complexes (Sharma et al., 2011; Wang and Tsang, 2013), which hinder its access to sorbent surface. On the other hand, increasing As mobility by organic surfactants provides a new way for As removal from contaminated soil (Gusiatin, 2014).

Though the effects of single ions have been widely studied in batch systems, their combined impacts on As adsorption and transport in field columns are still not fully understood. The complexity of the coexisting ion effects can be manifested by HCO_3^-, which competes weakly with As adsorption, but may greatly promote the release of adsorbed As in the presence of

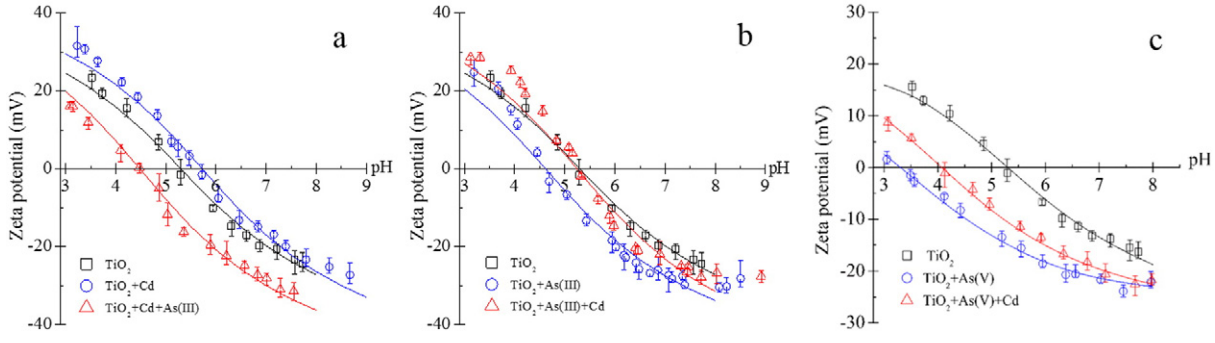

Fig. 6 – Experimental and CD-MUSIC simulations of zeta potential of 0.2 g/L TiO_2 as a blank, 0.03 mmol/L As(III)/As(V), and 0.03 mmol/L Cd adsorbed TiO_2 as a function of pH in 0.04 mol/L $NaClO_4$ solution (Hu et al., 2015b). (a) The pHpzc of TiO_2 with Cd adsorbed first and then As(III) was added to the system. (b) The pHpzc of TiO_2 with As(III) adsorbed first and then Cd was added to the system. (c) The pHpzc of TiO_2 with As(V) adsorbed first and then Cd was added to the system.

Ca and Mg (Saalfield and Bostick, 2010). Cui et al. (2015a) studied the compounding influence of Ca, Mg, Si, and HCO_3^- on As removal by TiO_2, and found that the effect exhibited by coexisting ions was not a simple summation of individual ion effects but a compromise between them. By considering the compounding effects of Si, Ca, and HCO_3^- on As adsorption, the As breakthrough curves in TiO_2 field columns were successfully predicted (Hu et al., 2015a).

The effects that coexisting ions have on As removal are significant and inevitable to consider when studying actual groundwater especially those contributed by Si and Ca, which exist at much higher concentrations in groundwater. When seeking improved As removal technology, it is critical to accurately quantify and predict the competitive interactions of As with ions coexisting on oxide surfaces. Studying molecular surface complexes in the presence of coexisting ions during filtration may contribute to successful modeling of the geochemical transport.

2. Connection of batch adsorption experiments with field filtration

Comprehensive study for treatment of As in water combining oxidation, coagulation, and filtration is reported by previous publications (Cui et al., 2015b; Terracciano et al., 2015), and filtration adsorption is considered one of the most cost-effective and user-friendly techniques that provide As-treated water worldwide (Bang et al., 2005; Cui et al., 2015a; Hu et al., 2015a). Adsorptive filtration using TiO_2 fixed-bed columns for As removal has been reported by extensive studies (Table 2). Bang et al. (2005) used a granular TiO_2 column to treat groundwater with an As concentration of 43 μg/L. Hristovski et al. (2007, 2008) used aggregated TiO_2 nanoparticles and titanate nanofibers as packed bed adsorbent media to treat As(V)-contaminated water with concentrations ranging from 28 to 122 μg/L. As part of a current study, two different samples of geogenic groundwater were taken from sites in Shanxi, China; the first contained 374 μg/L As(III) and 291 μg/L As(V), and the second had 454 μg/L As(III) and 88 μg/L As(V). These water samples were remediated using granular TiO_2 columns, and their results suggested that groundwater treatment using TiO_2 can provide As-safe drinking water (Fig. 7) (Cui et al., 2015a; Hu et al., 2015a). Accurate predictions of As breakthrough curves from filtration columns are important to determine and plan for future operating and maintenance costs. Therefore, simulating As breakthrough curves using parameters from batch adsorption experiments is a key issue in need of a solution.

2.1. Field columns with various empty bed contact time

Empty bed contact time (EBCT) is considered a major connection between batch adsorption and column filtration, also a significant parameter that controls As breakthrough curves from fixed-bed columns. General understanding is that extended As removal can be achieved with a long EBCT (Hristovski et al., 2007, 2008; Kanematsu et al., 2012). For example, the study of Hristovski et al. (2007) suggested that arsenic breakthrough (>1 μg/L) on titanium-based Adsorbsia GTO columns began at 3000, 6000, and 10,000 bed volumes (BVs) with EBCTs of 0.1, 0.25, and 0.5 min. Similarly, Cui et al. (2015a) studied the As breakthrough curves on granular TiO_2 columns at EBCTs of 0.11, 0.22, 0.32, 0.54, and 1.08 min, and the results indicated that the number of BV before the effluent As concentration exceeded 10 μg/L (BV_{10}) exhibited a clear linear increase as a function of EBCT. The reason can be attributed to the fact that extended contact time can facilitate the mass transfer diffusion of As into granular TiO_2 pores (Cui et al., 2015a), which can also be evidenced by the As reaction constant log*K* increasing as a function of adsorption time (Swedlund et al., 2014).

However, Westerhoff et al. (2006) theorized that improved arsenic removal can be achieved with a shorter EBCT on goethite-based granular porous adsorbent E33, because competing constituents (*e.g.*, silicate) migrate more quickly through the bed than As (Cui et al., 2015a), and with a longer EBCT there is a longer exposure to competing ions and therefore less treatability than at a shorter EBCT. Similar results were also observed by Kanematsu et al. (2012). They showed that a longer EBCT resulted in a worse As(V) removal performance with iron oxide in the presence of Si, because Si moves faster than As(V) and occupies adsorption sites on the media. In addition, an extended EBCT could increase time cost during the water treatment process. Therefore, the set of EBCT necessitates careful study by considering the effect of coexisting ions and economic factors.

2.2. PHREEQC coupled with CD-MUSIC to simulate As transport in the field column

Arsenic adsorption on metal oxide surfaces has been extensively studied using varied surface complexation models (Kanematsu et al., 2013; Stachowicz et al., 2008). CD-MUSIC is one of the most widely used models to describe As adsorption behavior on metal oxide surfaces under the constraint of synchrotron spectroscopic studies and molecular simulation results (Cui et al., 2015a; Hu et al., 2015b). PHREEQC, a geochemical model, integrates a macroscopic mass transfer process with a microscopic surface complexation model (Parkhurst and Appelo, 2013). It can be applied in calculating solution complex speciation, batch-reaction, one-dimensional reactive-transport, and inverse modeling.

CD-MUSIC models were used to simulate batch adsorption behaviors of As(III), As(V), and coexisting ions such as Ca, Si, and HCO_3^- at the TiO_2 surface (Cui et al., 2015a; Hu et al., 2015a). In the modeling runs, the transport properties of groundwater components and adsorption constants remained the same except for some fine-tuning of As adsorption parameters in the CD-MUSIC model. When using this fine-tuning approach, the parameters obtained from batch adsorption must be modified to satisfactorily approximate the column data. Kinetic limitations were initially thought to be the critical contributor in predicting the As transport process in the TiO_2 columns using parameters obtained with batch experiments (Hu et al., 2015a; Maji et al., 2012); however, after excluding their influence, the effect of coexisting ions on As adsorption was recognized as the main challenge. Herein, while simultaneously considering the adsorptions of As, Ca^{2+}, $Si(OH)_4$, and HCO_3^-, and the formation of Ca–As–TiO_2 ternary surface complexes, the breakthrough curves of As, Ca^{2+}, $Si(OH)_4$, and HCO_3^- in the TiO_2 filters were well-simulated with the PHREEQC

Table 2 – Summary of As removal from geogenic groundwater and wastewater using column filtration.

TiO_2 media	Particle size (mm)	EBCT (min)	BV_{10}	Reaction conditions	$q(BV_{10})$ (mg/g)	Reference
Granular TiO_2	0.15–0.6	3	45000	As(V) = 43 μg/L, Ca = 41 mg/L, Mg = 26 mg/L, Si = 21 mg/L, HCO_3^- = 210 mg/L, pH = 7.91	1.7	Bang et al. (2005)
Granular TiO_2	0.15–0.6	3	41500	As(V) = 52 μg/L, Ca = 41 mg/L, Mg = 26 mg/L, Si = 21 mg/L, pH = 7.67–8.36	2.8	Bang et al. (2011)
Granular TiO_2	0.18–0.38	2.5	3460	As(III) = 56 μg/L, As(V) = 14 μg/L, Ca = 36 mg/L, Mg = 16 mg/L, Si = 33 mg/L, P = 20 μg/L, pH = 7.3	0.29	Hao et al. (2009)
Granular TiO_2	0.38–0.83	0.11	0	As(III) = 373 μg/L, As(V) = 291 μg/L, Ca = 39.1 mg/L, Mg = 104.3 mg/L, Si = 8.9 mg/L, HCO_3^- = 387.5 mg/L, pH = 8.2	0	Cui et al. (2015a)
		0.22	158		0.13	
		0.32	247		0.18	
		0.54	527		0.40	
		1.08	968		0.96	
Granular TiO_2	0.18–0.25	4	2955	As(III) = 454 μg/L, As(V) = 88 μg/L, Ca = 35.3 mg/L, Mg = 24.6 mg/L, Si = 5.1 mg/L, pH = 8.2	1.53	Hu et al. (2015a)
		4	2563		1.36	
		4	2577		1.49	
		4	2392		1.38	
MetsorbG		0.48	21000	As(V) = 43 μg/L, Ca = 30 mg/L, Si = 3.7 mg/L, HCO_3^- = 87 mg/L, P = 15 μg/L, pH = 7.2	0.6	USEPA (2008)
MetsorbG		0.57	16000	As(V) = 21.5 μg/L, Ca = 54 mg/L, HCO_3^- = 342 mg/L, P = 54 μg/L, pH = 7.7	0.2	USEPA (2008)
MetsorbG		0.28	15000	As(V) = 28 μg/L, Si = 25 mg/L, pH = 8	0.51	Hristovski et al. (2007)
MetsorbG		5	14000	As(V) = 25 μg/L, pH = 7.8	0.2	Westerhoff et al. (2006)
Adsorbia GTO		0.57	4000	As(V) = 51 μg/L, Ca = 5.1 mg/L, Si = 10.7 mg/L, HCO_3^- = 83 mg/L, P = 162 μg/L, pH = 7.4	0.2	USEPA (2008)
Adsorbia GTO		0.48	16000	As(V) = 43 μg/L, Ca = 30 mg/L, Si = 3.7 mg/L, HCO_3^- = 87 mg/L, P = 15 μg/L, pH = 7.2	0.5	USEPA (2008)
Adsorbia GTO		0.38	12500	As(III) = 0.8 μg/L, As(V) = 40.2 μg/L, Ca = 18 mg/L, Si = 5.1 mg/L, HCO_3^- = 69 mg/L, P = 33 μg/L, pH = 8.6	0.4	USEPA (2008)
Adsorbia GTO		0.38	10000	As(III) = 22.5 μg/L, As(V) = 13 μg/L, Ca = 16 mg/L, Si = 5.1 mg/L, HCO_3^- = 64 mg/L, P = 24 μg/L, pH = 8.5		USEPA (2008)
Adsorbia GTO		0.1	5288	As(V) = 28 μg/L, Si = 25 mg/L, pH = 8	0.12	Hristovski et al. (2007)
		0.25	7755		0.07	
		0.28	29000		0.34	
		0.5	10575		0.09	
Granular TiO_2	0.25–0.38	30	90	As(III) = 2590 ± 295 mg/L, Cd = 12 ± 2 mg/L, pH = 7.0	162 ± 20	Yan et al. (2015)

EBCT: empty bed contact time. BV_{10}: bed volume before As effluent concentration below 10 μg/L. $q(BV_{10})$: As adsorption density when the effluent As concentration was <10 μg/L.

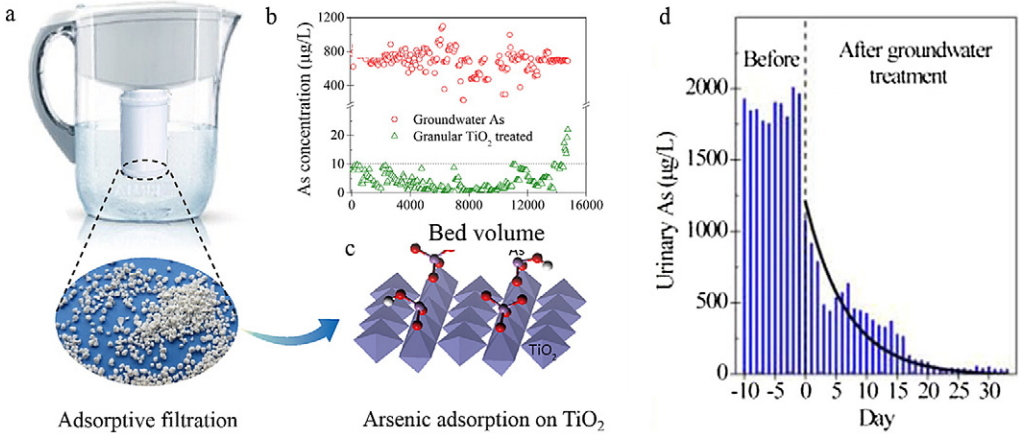

Fig. 7 – (a) Household filter using granular TiO_2 as adsorbent media. (b) As breakthrough curve from a filter as a function of bed volumes. (c) Arsenic adsorption structures on TiO_2 as evidenced by EXAFS study (Cui et al., 2015a). (d) Urinary As concentration decreased after local residents drank As-treated groundwater (Hu et al., 2015a). EXAFS: extended X-ray absorption fine structure.

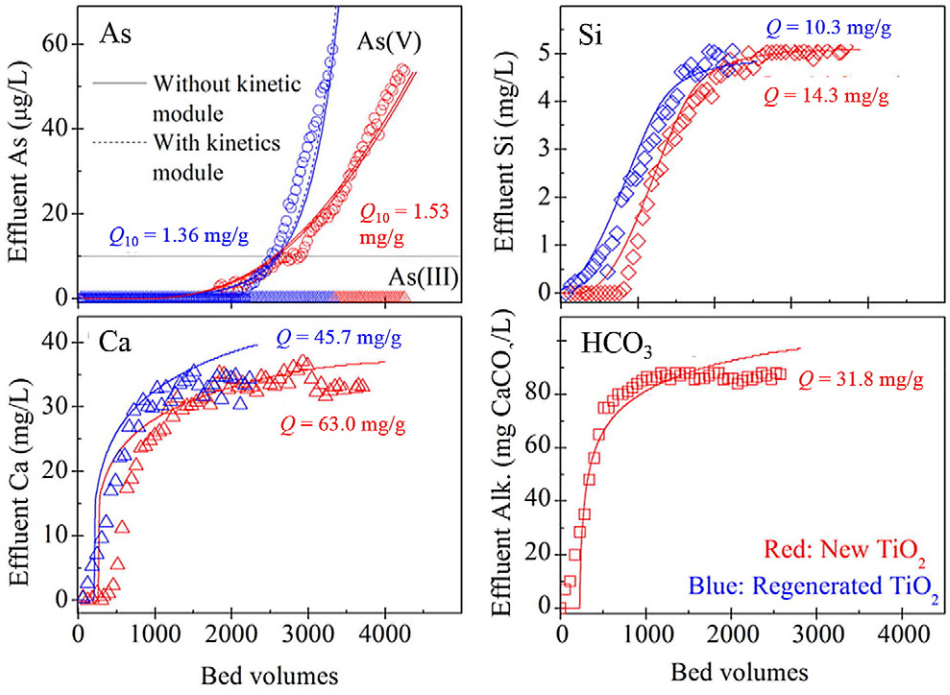

Fig. 8 – Observed (points) and simulated (lines) for As, $Si(OH)_4$, Ca^{2+}, and HCO_3^- breakthrough curves with 10 g of new (red) and regenerated (blue) granular TiO_2 as a function of bed volumes during the filtration experiments. The dashed lines in As breakthrough curves are PHREEQC modeling results with the inclusion of a kinetics module. Q represents the total adsorption capacities during the column filtration experiments, while Q_{10} is the As adsorption capacity when the effluent As concentration was <10 μg/L (Hu et al., 2015a).

model (Fig. 8) (Hu et al., 2015a). The satisfactory modeling results endorse the application of CD-MUSIC in the PHREEQC code to predict As adsorptive transport in the TiO_2 columns, and highlight the importance of compounding ion effects on As adsorption.

3. Regeneration and reuse of TiO_2

The regeneration and reuse of spent TiO_2 media presents a pressing issue for its application as an efficient adsorbent. Following As adsorption, it is usually regenerated with NaOH (Arumugam et al., 2013; Hu et al., 2015a). For a typical study using granular TiO_2 to remediate wastewater with a high concentration of As(III) and coexisting Cd (Yan et al., 2015), spent TiO_2 media were regenerated using H_2SO_4 and NaOH. The total desorption ratio was in the ranges of 76%–93% for As(III) and 62%–89% for Cd in 10 treatment cycles, and the regenerated TiO_2 adsorbent was able to be re-used with no decrease in its adsorption capacity, which was 162 ± 20 mg/g for As(III) and 1.00 ± 0.16 mg/g for Cd.

For TiO_2 that adsorbs groundwater containing As and coexisting Si, the formation of Si polymers can occupy the surface sites and consequently inhibit As adsorption and TiO_2 regeneration (Christl et al., 2012; Hu et al., 2015c). Hu et al. (2015a) studied granular TiO_2 regeneration using NaOH and HCl after adsorbing real groundwater containing the following analytes of interest at pH 8.2: 454 μg/L As(III), 88 μg/L As(V), 35.3 mg/L Ca, and 5.10 mg/L Si. The As desorption rate was able to reach 99.5% for the first regeneration and 98.7% for the second, and the adsorption capacities of the TiO_2 column before the effluent As concentration exceeded 10 μg/L was 1.53 and 1.36 mg/g for pristine and regenerated TiO_2, respectively. The desorption rates were 86.8%–88.6% for Ca^{2+} and 45.9%–48.2% for $Si(OH)_4$. The low $Si(OH)_4$ desorption rate can be ascribed to the polymerization of $Si(OH)_4$ on the TiO_2 surface during the long-term filtration cycle (Hu et al., 2015c). With the formation of $Si(OH)_4$ polymers and because of their low desorption rates, decreased As adsorption capacities in the regenerated TiO_2 column were observed, even though the As regeneration rate was extremely high (98.7%–99.5%) (Hu et al., 2015a).

4. Perspectives

Regeneration of spent TiO_2 media presents an enduring topic for promoting the application of TiO_2 in practice. Due to the formation of $Si(OH)_4$ surface oligomers and polymers on the TiO_2 surface, the presence of silicates in the groundwater may be one of the most important reasons for the exhaustion of the As adsorption capacity. In order to use and regenerate TiO_2 adsorbents efficiently, groundwater filtration must be completed in a short period of time (or a short EBCT) before Si oligomer and polymer species colonize TiO_2 surface sites.

Meanwhile, appropriate generation approaches should be developed to remove surface silicate oligomers and polymers during the adsorbent regeneration process. Furthermore, studies concerning the post-treatment of the regeneration solution would be beneficial.

The substantial development of TiO_2-based materials has made adsorptive filtration a promising technology for arsenic removal in the future. Thus, synthesizing TiO_2-based materials with an excellent adsorption performance is a consistent pursuit. Meanwhile, TiO_2 material should have a large particle size and strong hardness to be operated easily in field filtration. Recent studies have shown that the adsorption performance of TiO_2 largely depends on its exposed crystal facets (Liu et al., 2014; Yan et al., 2016). The study of As adsorption on different anatase TiO_2 surfaces suggests that {001} facets have stronger Lewis acid sites than {101} facets, resulting in a higher As adsorption affinity, with As surface complexes being more energetically favorable on {001} than on {101} facets (Yan et al., 2016). Thus, TiO_2 with highly-active {001} facets should present a favorable adsorption to As. Although much effort has been put into fabricating TiO_2 with more exposed {001} facets, the synthesized TiO_2 exhibits a limited specific surface area of 1.6 m^2/g (Yang et al., 2009). Thus, the synthesis of TiO_2 with more exposed active facets and large surface areas is another direction in which to endeavor.

TiO_2-based arsenic removal methods developed to date have been mainly focused on the photocatalytic oxidation of As(III) to As(V), followed by adsorption due to the lower affinity of As(III) to metal oxide surfaces. Photooxidation of As(III) in UV/TiO_2 systems has been extensively studied. However, the mechanisms of As(III) photocatalytic oxidation on TiO_2 is still a controversy, which is proposed to be controlled by different reactive oxygen species such as the hydroxyl radical (.OH) and superoxide radical ($O_2.^-$) (Ding et al., 2015; Dutta et al., 2005; Ryu and Choi, 2006). Many efforts have been taken to synthesize TiO_2 with active {001} facets, which is preferred in the generation of .OH (Liu et al., 2010). Another study concludes that {001} facets can facilitate the transfer of photo-excited electrons to the adsorbed O_2 to generate $O_2.^-$ (Yan et al., 2016), which contributes to As(III) photooxidation. Further studies suggest that the synergy of low-energy {101} and high-energy {001} TiO_2 facets can enhance the photocatalytic activity of anatase TiO_2 with the spatial separation of reduction and oxidation sites in different TiO_2 facets (Roy et al., 2013; Yu et al., 2014). Therefore, the synergistic effects of different coexisting facets on the generation of radicals, and their influence on the As(III) photocatalytic oxidation process should be elucidated in the future. Understanding these phenomena is essential to the application of TiO_2 in the arsenic water treatment field.

Acknowledgments

This work was supported by the National Basic Research Program (973) of China (No. 2015CB932003), the Strategic Priority Research Program of the Chinese Academy of Sciences (No. XDB14020201), and the National Natural Science Foundation of China (Nos. 41373123, 41425016, and 21321004).

REFERENCES

Arumugam, A., Ponnusami, V., Narendhar, C., Bhuvaneshvari, T.S., 2013. Novel waste water treatment strategy using titanate nanofibers in fixed bed reactor. In: Giri, P.K., Goswami, D.K., Perumal, A. (Eds.), Advanced Nanomaterials and Nanotechnology, pp. 589–598.

Bang, S., Patel, M., Lippincott, L., Meng, X.G., 2005. Removal of arsenic from groundwater by granular titanium dioxide adsorbent. Chemosphere 60, 389–397.

Bang, S., Pena, M.E., Patel, M., Lippincott, L., Meng, X., Kim, K.W., 2011. Removal of arsenate from water by adsorbents: a comparative case study. Environ. Geochem. Health 33, 133–141.

Bian, Z., Miao, X., Lei, S., Chen, S., Wang, W., Struthers, S., 2012. The challenges of reusing mining and mineral-processing wastes. Science 337, 702–703.

Chen, X., Mao, S.S., 2007. Titanium dioxide nanomaterials: synthesis, properties, modifications, and applications. Chem. Rev. 107, 2891–2959.

Christl, I., Brechbuehl, Y., Graf, M., Kretzschmar, R., 2012. Polymerization of silicate on hematite surfaces and its influence on arsenic sorption. Environ. Sci. Technol. 46, 13235–13243.

Ciardelli, M.C., Xu, H., Sahai, N., 2008. Role of Fe(II), phosphate, silicate, sulfate, and carbonate in arsenic uptake by coprecipitation in synthetic and natural groundwater. Water Res. 42, 615–624.

Cui, J., Du, J., Yu, S., Jing, C., Chan, T., 2015a. Groundwater arsenic removal using granular TiO_2: integrated laboratory and field study. Environ. Sci. Pollut. Res. 22, 8224–8234.

Cui, J., Jing, C., Che, D., Zhang, J., Duan, S., 2015b. Groundwater arsenic removal by coagulation using ferric(III) sulfate and polyferric sulfate: a comparative and mechanistic study. J. Environ. Sci. 32, 42–53.

Deng, S., Li, Z., Huang, J., Yu, G., 2010. Preparation, characterization and application of a Ce–Ti oxide adsorbent for enhanced removal of arsenate from water. J. Hazard. Mater. 179, 1014–1021.

Ding, W., Wang, Y., Yu, Y., Zhang, X., Li, J., Wu, F., 2015. Photooxidation of arsenic(III) to arsenic(V) on the surface of kaolinite clay. J. Environ. Sci. 36, 29–37.

Dutta, P.K., Ray, A.K., Sharma, V.K., Millero, F.J., 2004. Adsorption of arsenate and arsenite on titanium dioxide suspensions. J. Colloid Interface Sci. 278, 270–275.

Dutta, P.K., Pehkonen, S.O., Sharma, V.K., Ray, A.K., 2005. Photocatalytic oxidation of arsenic(III): evidence of hydroxyl radicals. Environ. Sci. Technol. 39, 1827–1834.

Dwivedi, C., Raje, N., Nuwad, J., Kumar, M., Bajaj, P.N., 2012. Synthesis and characterization of mesoporous titania microspheres and their applications. Chem. Eng. J. 193, 178–186.

Grafe, M., Nachtegaal, M., Sparks, D.L., 2004. Formation of metal-arsenate precipitates at the goethite-water interface. Environ. Sci. Technol. 38, 6561–6570.

Grafe, M., Beattie, D.A., Smith, E., Skinner, W.M., Singh, B., 2008. Copper and arsenate co-sorption at the mineral-water interfaces of goethite and jarosite. J. Colloid Interface Sci. 322, 399–413.

Guan, X.H., Du, J.S., Meng, X.G., Sun, Y.K., Sun, B., Hu, Q.H., 2012. Application of titanium dioxide in arsenic removal from water: a review. J. Hazard. Mater. 215, 1–16.

Guo, J.W., Cai, X.J., Li, Y., Zhai, R.G., Zhou, S.M., Na, P., 2013. The preparation and characterization of a three-dimensional titanium dioxide nanostructure with high surface hydroxyl group density and high performance in water treatment. Chem. Eng. J. 221, 342–352.

Gusiatin, Z.M., 2014. Tannic acid and saponin for removing arsenic from brownfield soils: mobilization, distribution and speciation. J. Environ. Sci. 26, 855–864.

Hao, J., Han, M.-J., Wang, C., Meng, X., 2009. Enhanced removal of arsenite from water by a mesoporous hybrid material — thiol-functionalized silica coated activated alumina. Microporous Mesoporous Mater. 124, 1–7.
Hao, J., Han, M.-J., Han, S., Meng, X., Su, T.-L., Wang, Q.K., 2015. SERS detection of arsenic in water: a review. J. Environ. Sci. 36, 152–162.
Hristovski, K., Baumgardner, A., Westerhoff, P., 2007. Selecting metal oxide nanomaterials for arsenic removal in fixed bed columns: from nanopowders to aggregated nanoparticle media. J. Hazard. Mater. 147, 265–274.
Hristovski, K., Westerhoff, P., Crittenden, J., 2008. An approach for evaluating nanomaterials for use as packed bed adsorber media: a case study of arsenate removal by titanate nanofibers. J. Hazard. Mater. 156, 604–611.
Hu, S., Shi, Q.T., Jing, C.Y., 2015a. Groundwater arsenic adsorption on granular TiO_2: integrating atomic structure, filtration, and health impact. Environ. Sci. Technol. 49, 9707–9713.
Hu, S., Yan, L., Chan, T., Jing, C., 2015b. Molecular insights into ternary surface complexation of arsenite and cadmium on TiO_2. Environ. Sci. Technol. 49, 5973–5979.
Hu, S., Yan, W., Duan, J.M., 2015c. Polymerization of silicate on TiO_2 and its influence on arsenate adsorption: an ATR-FTIR study. Colloids Surf. A Physicochem. Eng. Asp. 469, 180–186.
Jegadeesan, G., Al-Abed, S.R., Sundaram, V., Choi, H., Scheckel, K.G., Dionysiou, D.D., 2010. Arsenic sorption on TiO_2 nanoparticles: size and crystallinity effects. Water Res. 44, 965–973.
Jiang, W., Lv, J., Luo, L., Yang, K., Lin, Y., Hu, F., Zhang, J., Zhang, S., 2013. Arsenate and cadmium co-adsorption and co-precipitation on goethite. J. Hazard. Mater. 262, 55–63.
Kanematsu, M., Young, T.M., Fukushi, K., Green, P.G., Darby, J.L., 2012. Individual and combined effects of water quality and empty bed contact time on As(V) removal by a fixed-bed iron oxide adsorber: implication for silicate precoating. Water Res. 46, 5061–5070.
Kanematsu, M., Young, T.M., Fukushi, K., Green, P.G., Darby, J.L., 2013. Arsenic(III, V) adsorption on a goethite-based adsorbent in the presence of major co-existing ions: modeling competitive adsorption consistent with spectroscopic and molecular evidence. Geochim. Cosmochim. Acta 106, 404–428.
Kocabas-Atakli, Z.O., Yurum, Y., 2013. Synthesis and characterization of anatase nanoadsorbent and application in removal of lead, copper and arsenic from water. Chem. Eng. J. 225, 625–635.
Ler, A., Stanforth, R., 2003. Evidence for surface precipitation of phosphate on goethite. Environ. Sci. Technol. 37, 2694–2700.
Liang, C., Wang, X., Peng, X., 2016. Arsenic retention and transport behavior in the presence of typical anionic and nonionic surfactants. J. Environ. Sci. 39, 249–258.
Liao, X., Li, Y., Yan, X., 2016. Removal of heavy metals and arsenic from a co-contaminated soil by sieving combined with washing process. J. Environ. Sci. 41, 202–210.
Liu, G., Sun, C., Yang, H.G., Smith, S.C., Wang, L., Lu, G.Q., Cheng, H.-M., 2010. Nanosized anatase TiO_2 single crystals for enhanced photocatalytic activity. Chem. Commun. 46, 755–757.
Liu, G., Yang, H.G., Pan, J., Yang, Y.Q., Lu, G.Q., Cheng, H.-M., 2014. Titanium dioxide crystals with tailored facets. Chem. Rev. 114, 9559–9612.
Luo, T., Cui, J., Hu, S., Huang, Y., Jing, C., 2010. Arsenic removal and recovery from copper smelting wastewater using TiO_2. Environ. Sci. Technol. 44, 9094–9098.
Maji, S.K., Kao, Y.-H., Wang, C.-J., Lu, G.-S., Wu, J.-J., Liu, C.-W., 2012. Fixed bed adsorption of As(III) on iron-oxide-coated natural rock (IOCNR) and application to real arsenic-bearing groundwater. Chem. Eng. J. 203, 285–293.
Masue, Y., Loeppert, R.H., Kramer, T.A., 2007. Arsenate and arsenite adsorption and desorption behavior on coprecipitated aluminum : iron hydroxides. Environ. Sci. Technol. 41, 837–842.
Miller, S.M., Zimmerman, J.B., 2010. Novel, bio-based, photoactive arsenic sorbent: TiO_2-impregnated chitosan bead. Water Res. 44, 5722–5729.
Nabi, D., Aslam, I., Qazi, I.A., 2009. Evaluation of the adsorption potential of titanium dioxide nanoparticles for arsenic removal. J. Environ. Sci. 21, 402–408.
Nilchi, A., Garmarodi, S.R., Darzi, S.J., 2011. Removal of arsenic from aqueous solutions by an adsorption process with titania-silica binary oxide nanoparticle loaded polyacrylonitrile polymer. J. Appl. Polym. Sci. 119, 3495–3503.
Niu, H.Y., Wang, J.M., Shi, Y.L., Cai, Y.Q., Wei, F.S., 2009. Adsorption behavior of arsenic onto protonated titanate nanotubes prepared via hydrothermal method. Microporous Mesoporous Mater. 122, 28–35.
Parkhurst, D.L., Appelo, C.A.J., 2013. Description of Input and Examples for PHREEQC Version 3—A Computer Program for Speciation, Batch-Reaction, One-dimensional Transport, and Inverse Geochemical Calculations. U.S. Geological Survey.
Pena, M.E., Korfiatis, G.P., Patel, M., Lippincott, L., Meng, X.G., 2005. Adsorption of As(V) and As(III) by nanocrystalline titanium dioxide. Water Res. 39, 2327–2337.
Pirila, M., Martikainen, M., Ainassaari, K., Kuokkanen, T., Keiski, R.L., 2011. Removal of aqueous As(III) and As(V) by hydrous titanium dioxide. J. Colloid Interface Sci. 353, 257–262.
Roussel, C., Neel, C., Bril, H., 2000. Minerals controlling arsenic and lead solubility in an abandoned gold mine tailings. Sci. Total Environ. 263, 209–219.
Roy, N., Sohn, Y., Pradhan, D., 2013. Synergy of low-energy {101} and high-energy {001} TiO_2 crystal facets for enhanced photocatalysis. ACS Nano 7, 2532–2540.
Ryu, J., Choi, W., 2006. Photocatalytic oxidation of arsenite on TiO_2: understanding the controversial oxidation mechanism involving superoxides and the effect of alternative electron acceptors. Environ. Sci. Technol. 40, 7034–7039.
Saalfield, S.L., Bostick, B.C., 2010. Synergistic effect of calcium and bicarbonate in enhancing arsenate release from ferrihydrite. Geochim. Cosmochim. Acta 74, 5171–5186.
Sharma, P., Rolle, M., Kocar, B., Fendorf, S., Kappler, A., 2011. Influence of natural organic matter on As transport and retention. Environ. Sci. Technol. 45, 546–553.
Stachowicz, M., Hiemstra, T., van Riemsdijk, W.H., 2008. Multi-competitive interaction of As(III) and As(V) oxyanions with Ca^{2+}, Mg^{2+}, PO_4^{3-}, and CO_3^{2-} ions on goethite. J. Colloid Interface Sci. 320, 400–414.
Sun, Y.K., Zhou, G.M., Xiong, X.M., Guan, X.H., Li, L.N., Bao, H.L., 2013. Enhanced arsenite removal from water by $Ti(SO_4)_2$ coagulation. Water Res. 47, 4340–4348.
Swedlund, P.J., Holtkamp, H., Song, Y., Daughney, C.J., 2014. Arsenate–ferrihydrite systems from minutes to months: a macroscopic and IR spectroscopic study of an elusive equilibrium. Environ. Sci. Technol. 48, 2759–2765.
Terracciano, A., Ge, J., Meng, X., 2015. A comprehensive study of treatment of arsenic in water combining oxidation, coagulation, and filtration. J. Environ. Sci. 36, 178–180.
Urbano, B.F., Villenas, I., Rivas, B.L., Campos, C.H., 2015. Cationic polymer–TiO_2 nanocomposite sorbent for arsenate removal. Chem. Eng. J. 268, 362–370.
USEPA, 2008. Assessing Arsenic Removal by Metal (Hydr)Oxide Adsorptive Media Using Rapid Small Scale Column Tests. Govenrnment Printing Office, Washington, DC.
Wang, Y., Tsang, D.C.W., 2013. Effects of solution chemistry on arsenic(V) removal by low-cost adsorbents. J. Environ. Sci. 25, 2291–2298.
Westerhoff, P., De Haan, M., Martindale, A., Badruzzaman, M., 2006. Arsenic adsorptive media technology selection strategies. Water Qual. Res. J. Can. 41, 171–184.
Wu, S.L., Hu, W.T., Luo, X.B., Deng, F., Yu, K., Luo, S.L., Yang, L.X., Tu, X.M., Zeng, G.S., 2013. Direct removal of aqueous As(III) and As(V) by amorphous titanium dioxide nanotube arrays. Environ. Technol. 34, 2285–2290.

Xu, Z.H., Meng, X.G., 2009. Size effects of nanocrystalline TiO_2 on As(V) and As(III) adsorption and As(III) photooxidation. J. Hazard. Mater. 168, 747–752.

Xu, Z.C., Li, Q., Gao, S.A., Shang, J.K., 2010. As(III) removal by hydrous titanium dioxide prepared from one-step hydrolysis of aqueous $TiCl_4$ solution. Water Res. 44, 5713–5721.

Yan, L., Huang, Y., Cui, J., Jing, C., 2015. Simultaneous As(III) and Cd removal from copper smelting wastewater using granular TiO_2 columns. Water Res. 68, 572–579.

Yan, L., Du, J., Jing, C., 2016. How TiO_2 facets determine arsenic adsorption and photooxidation: spectroscopic and DFT study. Catal. Sci. Technol. 6, 2419–2426.

Yang, H.G., Liu, G., Qiao, S.Z., Sun, C.H., Jin, Y.G., Smith, S.C., Zou, J., Cheng, H.M., Lu, G.Q., 2009. Solvothermal synthesis and photoreactivity of anatase TiO_2 nanosheets with dominant {001} facets. J. Am. Chem. Soc. 131, 4078–4083.

Yu, J., Low, J., Xiao, W., Zhou, P., Jaroniec, M., 2014. Enhanced photocatalytic CO_2-reduction activity of anatase TiO_2 by coexposed {001} and {101} facets. J. Am. Chem. Soc. 136, 8839–8842.

Zhang, L., Yang, H., Tang, J., Qin, X., Yu, A.Y., 2014. Attenuation of arsenic in a karst subterranean stream and correlation with geochemical factors: a case study at Lihu, South China. J. Environ. Sci. 26, 2222–2230.